

# Stability of Continuous Emulsion Polymer Reactors

ANTHONY S. T. CHIANG and ROBERT W. THOMPSON,\* *Department of Chemical Engineering, Worcester Polytechnic Institute, Worcester, Massachusetts 01609*

## Synopsis

The stability of continuous emulsion polymer reactors having steady feed streams was studied. Analysis of a population balance model supported the notion of micelle deprivation as the chief cause of reactor instabilities. Analysis of the moments of the distribution indicated that the system may be uniquely stable in one case. Only one steady-state operating point was predicted for the case where the decrease in the termination rate constant due to the gel effect was neglected.

## INTRODUCTION

The mechanistic description of emulsion polymerization was first presented by Harkins.<sup>1</sup> Shortly thereafter Smith and Ewart<sup>2</sup> introduced a mathematical representation of the emulsion polymerization process based on Harkin's original concepts. They solved their recursion relation for three limiting cases. The most widely discussed solution is their case II kinetics, where free radical desorption does not occur and the free radical termination process is very rapid relative to the radical adsorption mechanism. The consequences of these conditions are that the average number of radicals per particle is  $\frac{1}{2}$ , or that at any time half of the particles contain a single growing polymer chain, while the other half contain none. The understanding of the process has been advanced far beyond these early theories. The reader is referred to the review article by Ugelstad and Hansen<sup>3</sup> and the treatise by Blackley<sup>4</sup> for thorough discussions of the kinetics of emulsion polymerization.

Gershberg and Longfield<sup>5</sup> presented one of the first analyses of continuous emulsion polymerization. Their model, based on Smith–Ewart case II kinetics, agreed fairly well with data collected in their laboratories. There were, however, several unresolved issues from their study.

Sato and Taniyama<sup>6</sup> modeled the emulsion polymer process as though it was a series of bimolecular collisions occurring between the species in the system (free radicals, polymer particles, etc.). Their model did not incorporate variations in properties due to particle size. Sato and Taniyama<sup>7</sup> later showed how their model could be used to analyze the performance of a continuous emulsion polymer reactor. Thompson and Stevens<sup>8</sup> extended their concept to include the free radical desorption mechanism. The advantages, and limitations, of this simplistic bimolecular collision concept were discussed by Thompson and Stevens,<sup>8</sup> and are not repeated here.

The first generation of population balance models for continuous emulsion polymer reactors were those reported by DeGraff and Poehlein<sup>9</sup> and Stevens and Funderburk.<sup>10</sup> Their models involved a particle balance over the whole reactor

\* To whom correspondence should be addressed.

system and required a known relationship between the average number of radicals per particle  $\bar{n}$  and the system parameters. Their models could not conveniently include the desorption mechanism, due to the inherent complexity of an integral of modified Bessel functions which would have been required in their solution.

Recently, Min and Ray<sup>11</sup> and Thompson and Stevens<sup>12</sup> have developed distributed population balance models in which the free radical desorption mechanism was easily included. Analysis of the steady-state behavior of the continuous reaction was presented by Thompson and Stevens.<sup>12</sup>

Gershberg and Longfield<sup>5</sup> noted periodic behavior in their early experiments with the continuous emulsion polymerization of styrene. After a startup period, monomer conversion in the continuous reactor exhibited sustained oscillation of amplitude between 1–4% (conversion units) and a frequency between 5–10 residence times. These fluctuations were noted in the majority of their experiments. Particle size distributions were not determined.

Omi et al.<sup>13</sup> observed oscillatory behavior in their continuous reactor when polymerizing styrene in emulsion. They showed results of an analog computer simulation based on a model quite similar to the one proposed by Gershberg and Longfield.<sup>5</sup> They reached the following conclusions from their simulations: (1) decreasing  $S_{in}$  (or increasing  $I_{in}$ ) increases the tendency toward unstable performance, and (2) limit cycles result only when the calculated free soap concentration is negative. The effects of the residence time were not discussed. The distribution of particle sizes was not included. The relations between their experimental observations and simulation results were not discussed.

Some minor difficulty with reactor fluctuations was noted by Gerrens and Kuchner<sup>14</sup> in their continuous styrene polymerization. The periodic fluctuations apparently ceased when the monomer feed was more carefully regulated. In a later study, Ley and Gerrens<sup>15</sup> observed sustained oscillations in the surface tension of the reaction mixture when polymerizing styrene in emulsion. They showed that the oscillations were associated with nucleation of successive generations of particles. As an "older" generation of relatively large particles washed out of the reactor, a new generation of particles was nucleated as a result of the excess soap available. Ley and Gerrens<sup>15</sup> speculated the existence of multiple steady states and postulated that limit-cycle behavior resulted when conditions were such that several steady states could exist.

Berens<sup>16</sup> observed oscillatory behavior in the particle size distribution of a continuous vinyl chloride emulsion polymer reactor. The interesting feature of his study was that in all of his experiments, the monomer conversion appeared to be quite steady, while the particle size distribution was changing with time.

Greene et al.<sup>17</sup> studied the continuous emulsion polymerization of vinyl acetate and methyl methacrylate. They observed oscillatory behavior for both monomers under certain conditions. Both the monomer conversion and the particle size distributions were shown to exhibit unsteady behavior. Increasing either  $I_{in}$  or  $\tau$  increased the tendency toward unstable performance. The effect of  $S_{in}$  was not as clearly identified from their work. In later experiments, a plug flow reactor was used to nucleate particles to be fed continuously to their stirred tank reactor. This arrangement reduced the tendency toward unstable behavior but did not eliminate the phenomenon altogether for some conditions.

Chiang<sup>18</sup> studied the behavior of time-dependent equations based on the model

proposed by Sato and Taniyama.<sup>6,7</sup> He found the model was valid for small residence times when the product consisted of small particles. Unstable performance resulted when polymerization rates were sufficiently high to yield negative values of the effluent free soap concentration. Unfortunately, the model was not sufficient to adequately characterize the real system, because particle size variations were ignored, and the model equations did not include any relationship describing the competition between particle nucleation and growth.

The recent simulation by Kiparissides et al.<sup>19</sup> demonstrates the oscillatory behavior noted so frequently in continuous emulsion polymer experiments. They developed a population balance model based on polymer particle age distributions and successfully simulated the results reported by Greene et al.<sup>17</sup> They chose a specific growth rate expression, based on a particle surface area dependence. While they were able to simulate transient experimental results, they did not report having studied the conditions required for stable performance. Chiang and Thompson<sup>20</sup> recently extended the work of Kiparissides et al.<sup>19</sup> by converting their integrodifferential equations to a purely differential form. Simulations of the transient behavior of the continuous reactor were presented, but no attempt was made to predict criteria for the stability of the system.

Kirillov and Ray<sup>21</sup> recently presented results of a simulation of continuous emulsion polymer reactor performance. The model was developed out of the framework presented earlier by Min and Ray.<sup>11</sup> The results of the model were compared to the experimental data for the emulsion polymerization of methyl methacrylate presented by Greene et al.<sup>17</sup> While the comparison of steady-state monomer conversion results was fair, the model failed to simulate the results of some experiments where sustained oscillations had been observed. The situation was corrected by adding a new mechanism and adjusting the value of the polymerization rate constant. No fewer than 25 independent parameters were involved in the simulation. No particle size distribution results were shown.

The current study was undertaken to predict the occurrence of sustained oscillations in continuous emulsion polymer reactors and to understand the reasons for this behavior.

## THEORETICAL DEVELOPMENT

We begin by assuming steady flows of water, monomer, emulsifier, and initiator to a homogeneously mixed stirred tank reactor having a constant volume and temperature. We assume that there are no polymer particles in the feed and that all particles in the effluent stream were generated inside the reactor. If the function  $N(t, \theta) d\theta$  represents the concentration of polymer particles at time  $t$  having age between  $\theta$  and  $\theta + d\theta$ , the population balance pertinent to this class of particles is

$$\partial N(t, \theta) / \partial t + \partial N(t, \theta) / \partial \theta = -N(t, \theta) / \tau \quad (1)$$

(The reader is referred to the treatise by Randolph and Larson<sup>22</sup> for a thorough discussion of the development and use of population balance expressions.) With the boundary conditions

$$\begin{aligned} N(t, 0) d\theta &= B(t) d\theta \\ N(0, \theta) d\theta &= N_0(\theta) d\theta \end{aligned} \quad (2)$$

the solution of eq. (1) is

$$N(t, \theta) = \begin{cases} B(t - \theta)e^{-\theta/\tau} & \text{for } \theta \leq t \\ N_0(\theta - t)e^{-t/\tau} & \text{for } \theta \geq t \end{cases} \quad (3)$$

When the relevant properties of the latex are related to  $N(t, \theta)$ , the system performance can be examined. We must supply appropriate particle nucleation and growth functions before we can determine these latex properties. Gardon<sup>23</sup> and Fitch<sup>24</sup> demonstrated that a nucleation function of the following form adequately describes the rate of generation of new particles:

$$B(t) = R_0(S_{\text{eff}}\alpha_m/s_m) - R_1A_T \quad (4)$$

Equation (4) accounts for particle nucleation in monomer swollen micelles and nucleation by oligomeric precipitation. The term involving the polymer particle surface area describes the decrease in the nucleation rate as large particles grow and consume soap.

The volumetric growth rate of a group of emulsion polymer particles of the same age,  $\theta$ , was expressed as a function of the system parameters by Gardon<sup>23</sup>:

$$\frac{dv(\theta)}{d\theta} = \frac{k_p\rho_m\phi_m}{N_A\rho_p(1 - \phi_m)} \bar{n}(\theta) \quad (5)$$

The quantities  $v(\theta)$  and  $\bar{n}(\theta)$  represent the average volume and average number of radicals per particle for the class of particles having the same age. The cumulative values of these quantities, total particle volume, and overall average number of radicals per particle will be time dependent if the system is unstable.

We now introduce a semiempirical relation between the average number of radicals per particle  $\bar{n}(\theta)$  and the particle radius  $r(\theta)$  of the following form:

$$\bar{n}(\theta) = Kr(\theta)^z \quad (6)$$

where the value of  $z$  is restricted to  $0 \leq z \leq 3$ , as demonstrated by Ugelstad and Hansen.<sup>3</sup> Vanderhoff et al. showed experimentally that the value of  $z$  should fall between 2.0 and 2.5 for polystyrene latex particles. Poehlein and Vanderhoff<sup>26</sup> reexamined the data<sup>25</sup> available on latex particle growth and concluded that the explanation of particle size-dependent growth rates was couched in the size-dependent value of  $\bar{n}(\theta)$ . That is, they concluded that the other parameters in eq. (5) were fairly insensitive to particle size variations. Their conclusions indicated that values of  $z$  of 2.5 and 3.0 are consistent with theoretical predictions for water- and oil-soluble initiators, respectively. The recent work by Kiparissides et al.,<sup>19</sup> which was extended by Chiang and Thompson,<sup>20</sup> demonstrated that the volumetric growth rate of latex particles should be a particle surface area-dependent process. That is, the growth rate of the particles should depend on the second power of the particle size.

The function  $r(\theta)$  may be found for spherical particles by combining eqs. (5) and (6):

$$r(\theta)\delta^{(3-z)} = K_G\theta + r_0\delta^{(3-z)} \quad (7)$$

where  $K_G$  is a lumped parameter defined in the Appendix, and  $r_0$  is the radius of a primary particle having age of zero. [Note that if  $z = 3$ , the function  $r(\theta)$  would take on a slightly different form. The case where  $z = 3$  is discussed later using moments. What follows, then, is strictly valid for  $0 \leq z < 3$ .]

### Steady-State Solution with Monomer Droplets Present

Clearly, two very different environments are relevant to the emulsion polymerization process. If emulsified monomer droplets are present in the reaction mixture, the monomer content of the polymer particles is usually presumed to be constant at the thermodynamic saturation level. Gardon<sup>23</sup> discusses this concept extensively. At some intermediate conversion level, the emulsified monomer droplets disappear and polymerization continues to consume the residual monomer remaining in the particles. The polymerization rate becomes ever lower as the fraction of monomer in the polymer particles  $\phi_m$  decreases, if  $k_t$  is assumed constant.

In fact, once the monomer droplets have disappeared, the rate of polymerization may increase. The cause of this phenomenon, discussed by Friis and Hamielec,<sup>27</sup> results from the gel effect within each particle. As monomer is consumed within each particle and  $\phi_m$  drops toward zero, the mobility of the growing chains is reduced and the value of  $k_t$  decreases. The decrease in  $k_t$  results in an increase in  $\bar{n}(\theta)$ , since a given particle can then house a larger number of growing chains simultaneously. The consequence of this phenomenon is that the termination rate constant  $k_t$ , becomes implicitly dependent on the conversion level. For the sake of this work we have ignored this dependence and assumed that  $k_t$  is a constant for all conversions. We point this out now and will refer to the consequences of this assumption later. We justify the assumptions at this point in time by pointing out that (1) the mathematics at high conversions would be quite complicated if the conversion-dependent behavior of  $k_t$  were included, because (2) the only analysis of the gel effect-related  $k_t$  conversion relation thus far is an empirical power-law expression for which constants must be evaluated.

The steady-state particle nucleation function can be determined by specifying the particle surface area, a physical property of the latex (see the Appendix for details). The cumulative particle surface area (assuming a spherical geometry) is given by

$$A_T = \int_0^\infty 4\pi r(\theta)^2 N(t, \theta) d\theta \quad (8)$$

By combining eqs. (4), (7), and (8) and assuming steady-state conditions, one has (after some manipulation)

$$B_{ss} = R_0 S_{\text{eff}} a_m / s_m - 4\pi R_1 B_{ss} \int_0^\infty (K_G \theta + r_0^{(3-z)})^{2/(3-z)} e^{-\theta/\tau} d\theta \quad (9)$$

The solution is given by

$$B_{ss} = \frac{R_0 S_{\text{eff}} a_m / s_m}{1 + \lambda} \quad (10)$$

where  $\lambda$  is defined in the Appendix.

Once the appropriate choice of  $z$  [in eq. (6)] and the other physical constants are known, the parameters  $\lambda$ ,  $J$ , and  $K_G$  may be determined. The steady-state nucleation rate may then be found from eq. (10). Finally, other relevant properties of the latex may be calculated:

$$N_{ss}(\theta) = B_{ss} e^{-\theta/\tau} \quad (11)$$

$$N_T = \int_0^\infty N_{ss}(\theta) d\theta = B_{ss} \tau \quad (12)$$

$$A_T = 4\pi r_0^2 B_{ss} \tau J^{2/(3-z)} e^{1/J} \Gamma\left(\frac{5-z}{3-z}\right) \quad (13)$$

$$= \lambda B_{ss} / R_1 \quad (13')$$

$$V_T = v_0 B_{ss} \tau J^{3/(3-z)} e^{1/J} \Gamma\left(\frac{6-z}{3-z}\right) \quad (14)$$

$$R_{ss} = \int_0^\infty \left( \frac{k_p \rho_m \phi_m}{N_A M_w} \bar{n}(\theta) \right) B_{ss} e^{-\theta/\tau} d\theta \quad (15)$$

$$= \frac{\rho_p (1 - \phi_m)}{M_w \tau} V_T \quad (15')$$

$$X_{ss} = \frac{R_{ss} \tau}{M_{in}} \quad (16)$$

The latex properties above are cumulative properties. Properties characteristic of the particle size distribution may also be determined. Specifically, the steady-state particle size distribution, average radius, and standard deviation are given by

$$U(r) = B_{ss} e^{1/J} \exp\left(-\frac{(r/r_0)^{(3-z)}}{J}\right) \quad (17)$$

$$\bar{L} = \frac{\int_0^\infty r(\theta) N_{ss}(\theta) d\theta}{\int_0^\infty N_{ss}(\theta) d\theta} \quad (18)$$

$$= r_0 e^{1/J} J^{1/(3-z)} \Gamma\left(\frac{2-z}{3-z}\right) \quad (18')$$

$$\delta^2 = \frac{\int_0^\infty r(\theta)^2 N_{ss}(\theta) d\theta}{\int_0^\infty N_{ss}(\theta) d\theta} - \left( \frac{\int_0^\infty r(\theta) N_{ss}(\theta) d\theta}{\int_0^\infty N_{ss}(\theta) d\theta} \right)^2 \quad (19)$$

$$= r_0^2 e^{1/J} J^{2/(3-z)} \left\{ \Gamma\left(\frac{5-z}{3-z}\right) - \left[ \Gamma\left(\frac{4-z}{3-z}\right) \right]^2 e^{1/J} \right\} \quad (19')$$

The particle size distribution in the effluent streams  $U(r)$  are found by combining eqs. (7) and (11).

At this point the steady-state performance of the continuous emulsion polymer reactor with monomer droplets present is fully characterized. These results may not describe the actual situation, however, because emulsified monomer droplets sometimes disappear at moderate monomer conversion levels. Under such conditions, the polymer particles will contain less than the saturation level of monomer, and the rate of polymerization will be somewhat lower than the maximum value if  $k_t$  is assumed constant. Results for this condition follow.

### Steady-State Solution with No Monomer Droplets

It is necessary to know at what monomer conversion level the emulsified droplets disappear before proceeding with a steady-state analysis in that regime. We can make a good estimate of that conversion level by assuming that the organic monomer is so sparingly soluble in water that the amount of monomer in the water phase is a negligible portion of the whole. Then at the instant when all monomer droplets vanish and the particles are still saturated with monomer, the weight fraction of polymer in the particles  $f$  was given by Kiparissides et al.<sup>19</sup>:

$$f = \frac{\rho_p(1 - \phi_m)}{\rho_m \phi_m + \rho_p(1 - \phi_m)} \quad (20)$$

All the organic material in the reactor is now contained in the particles, and by conservation of mass, the value of  $f$  must be the critical conversion level where the droplets just disappear. The predicted value for styrene is about  $f = 0.44$ . Actual values of this critical conversion level may be somewhat less than the predicted value, due to the monomer "sink" provided by the water phase.

Regardless of the conversion level, as long as all the polymerizable monomer resides in the particles, the volume fraction of monomer in polymer is given by

$$\phi_m^H = MM_w / \rho_m V_T^H \quad (21)$$

where the superscript  $H$  is to remind the reader that monomer droplets no longer exist (high conversion). The monomer conversion may be easily related to the volume fraction of monomer in the particles by considerations similar to the notions leading to eq. (20):

$$X_{ss}^H = \frac{\rho_p(1 - \phi_m^H)}{\rho_m \phi_m^H + \rho_p(1 - \phi_m^H)} \quad (22)$$

Finally, the total volume of polymer particles in the latex is found from the inlet monomer feed concentration:

$$V_T^H = M_{in} M_w \left( \frac{X_{ss}^H}{\rho_p} + \frac{1 - X_{ss}^H}{\rho_m} \right) \quad (23)$$

The reader can verify that eqs. (21)–(23) are internally consistent.

The volume fraction of monomer in the polymer particles may be found for a real system from eq. (22) once a steady-state conversion level is known. The total particle volume can then be determined from eq. (23). If the real system admits to a steady state in the absence of monomer droplets, then  $\phi_m^H$  will be constant, and the properties of the reaction mixture may be characterized by the relationships developed in eqs. (11)–(19), with  $\phi_m$  replaced by  $\phi_m^H$ .

### Stability of Steady States with Monomer Droplets

We now turn our attention to the question of the stability of the continuous emulsion polymerization reactor, having steady feed streams containing no polymer particles. When monomer droplets exist in the reaction mixture, we assume that the flux of monomer to the particles is sufficiently rapid to maintain the saturation level of monomer in the particles; in short,  $\phi_m$  is constant. Second,

we assume a constant free radical concentration in the water phase, tantamount to a linearization of the system equations.

To begin, we identify a cumulative deviation variable for some characteristic property of the latex:

$$P'(t) = \int_0^t p(\theta)B'(t - \theta)e^{-\theta/\tau} d\theta \quad (24)$$

where the prime denotes the deviation from the steady-state condition [see the Appendix for the details of the development of  $P'(t)$ ]. Equation (24) is a convolution integral and may be transformed to the Laplace domain with respect to  $(t/\tau)$ :

$$\tilde{P}'(s) = \tilde{p}(s + 1)\tilde{B}'(s) \quad (25)$$

where the tilde denotes the transformed function. To proceed we must specify both the transient nucleation function  $B'(t)$  and the individual latex properties of interest  $p(\theta)$  in terms of the Laplace transform variable  $s$ .

The transient particle generation function was given by eq. (4). This expression is written in terms of the deviation from the steady-state condition as

$$B'(t) = \frac{R_0 S'_{\text{eff}} a_m}{s_m} - R_1 \int_0^t a(\theta)B'(t - \theta)e^{-\theta/\tau} d\theta \quad (26)$$

which, for spherical particles, becomes

$$B'(t) = \frac{R_0 S'_{\text{eff}} a_m}{s_m} - 4\pi R_1 \int_0^t (K_G \theta + r_0^{(3-z)})^{2/(3-z)} B'(t - \theta)e^{-\theta/\tau} d\theta \quad (27)$$

After taking the Laplace transform of eq. (27) with respect to  $(t/\tau)$ , and solving for  $\tilde{B}'(s)$  one has

$$\tilde{B}'(s) = \frac{(R_0 a_m / s_m) \tilde{S}'_{\text{eff}}(s)}{1 + \lambda e^{s/J} (s + 1)^a} \quad (28)$$

The quantity  $S_{\text{eff}}$  is related to the soap entering the system. A material balance for the soap gives

$$\frac{dS}{dt} = \frac{S_{\text{in}}}{\tau} - \frac{S}{\tau} \quad (29)$$

and the Laplace transform for the deviation of soap about the steady-state value is

$$\tilde{S}'(s) = \tilde{D}/(s + 1) \quad (30)$$

where  $D$  is some arbitrary disturbance. Now by assuming the last three terms on the right side of eq. (A9) are independent of time, we have

$$\tilde{S}'_{\text{eff}}(s) = \tilde{S}'(s) = \tilde{D}/(s + 1) \quad (31)$$

Finally, by combining eqs. (28) and (31), we have

$$\tilde{B}'(s) = \frac{(R_0 a_m / s_m) \tilde{D}}{(s + 1)[1 + \lambda e^{s/J} (s + 1)^a]} \quad (32)$$

Equation (32) describes the transient response of the nucleation mechanism to



some arbitrary disturbance  $D$  in the Laplace domain. We will show that the major cause of continuous emulsion polymer reactor instabilities is couched in this aspect or the process.

The functional form of eq. (32) can be represented by the block diagram shown in Fig. 1, where the particle growth process regulates the formation of new particles. Viewed in this light it is easy to understand how the growing polymer particle surface regulates the performance of the polymerizer by competing with the nucleation mechanism for the incoming soap. Randolph and Larson<sup>22</sup> noted similar behavior in continuous crystallizers.

Greene et al.<sup>17</sup> showed that nucleating particles in a tubular reactor prior to introducing the feed stream to the CSTR (continuous stirred tank reactor) minimized the unstable performance in the CSTR which they noted without the tubular reactor. The effect of the arrangement can be understood in terms of the discussion just presented. The tubular reactor serves to enhance nucleation. The feed stream to the CSTR then contains growth surface which serves to regulate the nucleation within the CSTR. In addition, the CSTR environment would contain less of the substances required for nucleation and that effect would be minimized in the CSTR. Thus the competition between the two mechanisms is minimized in favor of particle growth.

The stability of this self-regulating system may be analyzed by the open-loop transfer function  $G(s)$ , where

$$G(s) = \lambda e^{s/J} (s + 1)^a \tag{33}$$

By substituting  $i\omega$  for  $s$ , the phase lag and amplitude ratio for the transfer function are found

$$\Phi = (\omega/J) + a \tan^{-1}\omega \tag{34}$$

and

$$(AR) = \lambda(\omega^2 + 1)^{a/2} \tag{35}$$

We can guarantee local stability of the particle nucleation mechanism by staisfying  $(AR) < 1$  for all  $\omega$ . Keeping in mind that  $a$  is negative, we must satisfy

$$\lambda < 1 \tag{36}$$

to guarantee stable reactor operation. This criterion is the same for all values of  $z$ , and all other parameters as well.

While  $\lambda < 1$  guarantees stable reactor performance, the condition  $\lambda > 1$  does

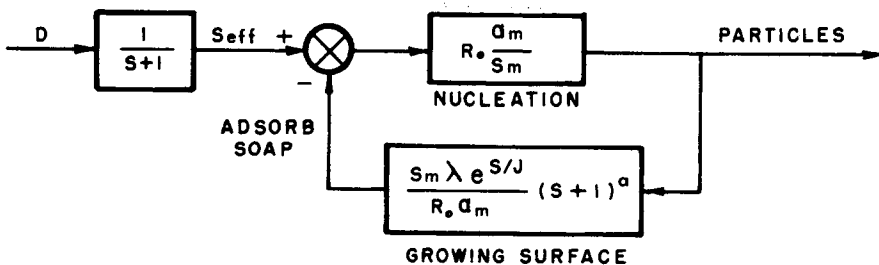


Fig. 1. Block diagram representation of regulation of particle nucleation by particle growth.

not assure unstable operation. Unstable operation would arise when  $\lambda > (\omega^2 + 1)^{-a/2}$ , where the value of  $\omega$  is determined from the solution of

$$a \tan^{-1}(\omega) + \omega/J = -\pi \quad (37)$$

Equation (37) does not admit to an analytical solution, and numerical approximations would depend on the choice of values for  $a$  and  $J$ . Due to the uncertainty in some of the physical constants, an exhaustive study of the critical values of  $\lambda$  for various  $a$  and  $J$  choices was not made. What follows is an analysis which is based on a guarantee of stability, and not instability.

We now return to our examination of the transient behavior of the other pertinent latex properties. Particle properties are related to the particle radius raised to a power,  $\xi$ :

$$p(\theta) = \phi_\xi r(\theta)^\xi \quad (38)$$

where  $\phi_\xi$  is a shape factor. The Laplace transform of eq. (38) with respect to  $\theta/\tau$ , using eq. (17), is

$$\tilde{p}(s) = \phi_\xi r_0^\xi J^{\xi/(3-z)} e^{s/J} \left( \frac{3-z+\xi}{3-z} \right) s^{-(3-z+\xi)/(3-z)} \quad (39)$$

Finally, a cumulative latex property related to the sum of the property of the particles is determined by combining eqs. (25), (32), and (39) and found, after some simplification, to be

$$\tilde{p}'_\xi(s) = \beta_\xi \frac{\lambda e^{s/J}}{(s+1)^{2+[\xi/(3-z)]} [1 + \lambda e^{s/J} (s+1)^a]} \quad (40)$$

where  $\beta_\xi$  is a constant whose value depends on  $\xi$  and is defined in the Appendix. The noteworthy feature of eq. (40) is that the part of the right-hand side essential to stable operation comes from the nucleation function. In addition, the stability of the particle generation mechanism will guarantee the stability of all other cumulative latex properties. Similarly, unstable particle generation behavior will necessarily result in unsteady latex properties.

The implications of the criterion set forth in eq. (36) regarding the distribution of soap molecules in the system can be understood by consideration of the cumulative steady-state particle surface area given by eq. (13). If particle nucleation occurs predominantly in the micelles available ( $h_n = 0$  and  $R_1 = R_0$ ), then eq. (13) can be transformed to

$$A_T = \frac{\lambda}{1+\lambda} \left( \frac{S_{\text{eff}}}{s_m} \right) a_0 \quad (41)$$

The quantity  $(S_{\text{eff}}/s_m)a_0$  represents the total effective surface area provided by the incoming soap,  $A_m$ . Thus the critical value of  $\lambda = 1$  yields

$$\frac{A_T}{A_m} = \frac{\lambda}{1+\lambda} \Big|_{\lambda=1} = \frac{1}{2} \quad (42)$$

which represents the critical fraction of the available organic-water interfacial area occupied by polymer particles. If the calculated steady-state particle surface area is less than  $1/2$  of the effective area of incoming soap, the system will be stable. This critical value will change if the criterion for stability is determined more rigorously.

### Stability of Steady States Without Monomer Droplets

When the emulsified monomer droplets vanish, the volume fraction of monomer in polymer is reduced from its saturated level, and  $\phi_m$  may be replaced by  $\phi_m^H$  as shown previously. We can say something quantitative about reactor stability at high conversions by assuming  $\phi_m^H$ , calculated for steady-state conditions, is constant during periods of unsteady performance. This assumption results in another linearization of the model equations. We justify this assumption by suggesting that for the type of oscillations reported experimentally (low amplitude, low frequency), the monomer fraction in the particles should change by 5% or less.

Since all lumped parameters are to be determined using a single value of  $\phi_m^H$ , the criterion for stability can be given by

$$\lambda^H < 1 \quad (43)$$

for the "not-so-rigorous" case or

$$\lambda^H < (\omega^2 + 1)^{-a/2} \quad (44)$$

and

$$a \tan^{-1}\omega + \omega/J^H = -\pi \quad (45)$$

for rigorous analysis.

### Stability Analysis by Moments

For some circumstances an analysis of the transient moment equations is sufficient to investigate stability and easier as well. The  $i$ th moment of the particle size distribution is defined as

$$M_i(t) = \int_0^\infty r^i U(t,r) dr \quad (46)$$

which may be normalized as

$$\mu_i(t) = \frac{1}{r_0^i} \int_0^\infty r^i U(t,r) dr \quad (47)$$

Now we write a population balance using particle radius as the distributed variable, instead of particle age:

$$\frac{\partial N}{\partial t} + \frac{\partial(NG)}{\partial r} = \frac{-N}{\tau} \quad (48)$$

By combining eqs. (5) and (6) and transforming the result to a radial basis, we have

$$G = \frac{dr}{dt} = \frac{K_G}{3-z} r^{z-2} \quad (49)$$

We consider here the situation where monomer droplets exist in the system and  $\phi_m$  is constant.

We can generate a closed set of moment equations by multiplying the resulting combination of eqs. (4), (48), and (49) by  $r^i$  and integrating over all particle sizes:

$$\frac{d\mu_0}{dT} = -\mu_0 + (a_0 R_0 \tau) \frac{S_{\text{eff}}}{s_m} - (a_0 R_1 \tau) \mu_2 \quad (50)$$

and

$$\frac{d\mu_i}{dT} = -\mu_i + i \left( \frac{J}{3-z} \right) \mu_{i+z-3} + (a_0 R_0 \tau) \frac{S_{\text{eff}}}{s_m} - (a_0 R_1 \tau) \mu_2 \quad (51)$$

where  $T = t/\tau$ .

The moment equations developed are useful for integer values of  $z$  only, for which case these relations are in fact similar to the integral equations developed earlier. The moment equations are valid, however, for  $z = 3$  without modification. Specifically, when  $z = 3$ , eqs. (50) and (51) become

$$\frac{d\mu_i}{dT} = (i\alpha - 1)\mu_i + \epsilon - \sigma\mu_2 \quad (52)$$

where  $i$  is allowed to take on integer values greater than or equal to zero.

The quantity  $(\epsilon - \sigma\mu_2)$  represents the particle nucleation rate, a function which is dependent on the cumulative particle surface area. This quantity is always nonnegative, being zero if no particles are being generated. If  $(\epsilon - \sigma\mu_2) = 0$ , intuition suggests that all latex properties, reflected in the zeroth to the third moments, ought to decrease with time. Thus all the coefficients  $(i\alpha - 1)$  should be less than zero. We can conclude from this argument, by considering the worst case of  $i = 3$ , that  $\alpha$  should be less than a value of  $1/3$ . For values of  $\alpha > 1/3$ , the cumulative latex particle volume can increase, even though no new particles are being generated. This situation by itself is not unreasonable, for it simply implies that particle growth is occurring in preference to particle nucleation. However, if  $(\epsilon - \sigma\mu_2) = 0$  and  $1/2 > \alpha > 1/3$ , then we are confronted with the curious problems of explaining how the cumulative particle volume can be increasing while the cumulative particle surface area is decreasing, all the while no new polymer particles are being created. The apparent solution to the dilemma posed above is to conclude that  $\alpha$  should take on values between zero (it must be positive) and  $1/3$  for the moment equations to adequately describe the real system.

The system of moment equations can be shown to be uniquely stable, or uniquely divergent, by solving the expression for  $\mu_2$  for arbitrary initial condition. The resulting expression converges to a steady-state operating point for

$$(2\alpha - 1 - \sigma) < 0 \quad (53)$$

and diverges unboundedly if the collection of terms is greater than or equal to zero. The real system would undoubtedly follow a trajectory to a high conversion level, such that monomer droplets disappear and the polymerization rate would regulate itself sufficiently to bring the system to rest at a steady-state operating point, or oscillate around a limit cycle. In short, the system would not diverge indefinitely, but be bounded by other constraints not considered here or eliminated during linearization.

The significant consideration for stable performance has once again reduced to a matter of the cumulative particle surface area and the competition between nucleation and growth. This conclusion arises from the criterion presented in eq. (53). The nature of the moment equations generated for  $z = 3$  lead one to conclude that (1) if  $\mu_2$  is a stable function, the entire system will be stable; (2) if  $\mu_2$  is a divergent function, the system will probably seek a high conversion operating point or a limit cycle; and (3) for  $z = 3$ , the continuous emulsion polymer reactor may be uniquely stable.

## DISCUSSION

The relationships developed in the previous sections were used to generate numerical values of some of the relevant dependent variables. A thorough presentation of results for the complete range of parameter values would be quite lengthy, due to the large number of independent parameters ( $z, B_{ss}, r_0, \lambda, J, \dots$ ). Additionally, not much would be gained by presenting the reader with a deluge of numerical results. Thus only results sufficient to understand the use of the model equations are shown.

Figure 2 shows the nature of the steady-state cumulative particle size distribution based on particle radius for  $z = 2.5$ . The cumulative distribution is found by integrating eq. (17) from  $r_0$  to  $r$  for fixed  $z, J$ , and  $B_{ss}$ . Also shown for each curve is the standard deviation, calculated from eq. (19'). Note that increasing the value of  $J$  results in the production of larger particles and broader particle size distribution. These results make sense qualitatively, since  $J$  is proportional to the polymerization rate constant  $k_p$ , and the holding time  $\tau$ .

The dimensionless average particle radius  $\bar{L}/r_0$ , is shown as a function of the parameter  $J$  in Figure 3. The curves shown are for various values of the growth rate parameter  $z$  and were determined from the steady-state relation in eq. (18'). Note that the average steady-state particle radius increases with  $J$ , and increases dramatically with increasing values of  $z$ . Again, the increase in  $(\bar{L}/r_0)$  with  $J$  makes physical sense because of the dependence of  $J$  on  $k_p$  and  $\tau$ . The somewhat stronger dependence of  $(\bar{L}/r_0)$  on  $z$  also seems reasonable, since  $z$  is the exponent relating the volumetric growth rate to particle radius.

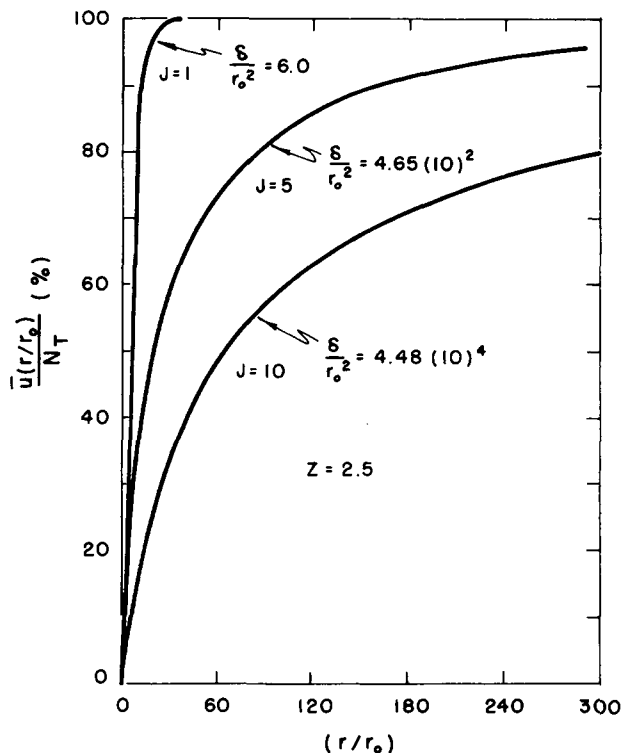


Fig. 2. Cumulative particle size distribution for various values of  $J$  at  $z = 2.5$ .

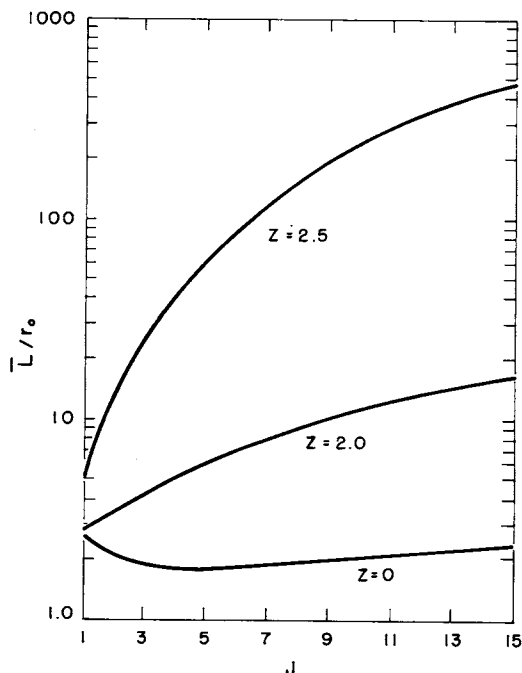


Fig. 3. Dependence of average particle radius on  $J$  for values of  $z$ .

Regions of stable and unstable reactor performance are shown in Figures 4 and 5 for values of  $z$  equal to 2.0 and 2.5, respectively. The curve describing the locus of points where  $\lambda = 1$  is shown crossing curves of constant  $\psi$  in these figures. In the region above this curve, the reactor is guaranteed to operate in a stable fashion. Points below this curve tend toward unstable behavior.

Some explanation of how the curves in Figures 4 and 5 were constructed is in order. The curves of constant  $\psi$  are the steady-state values of the rate ( $R_{ss}/M_{in}$ ) as a function of conversion ( $X_{ss}$ ). Given the values of the constants shown in the figures, the lines of constant  $\psi$  were found, when monomer droplets exist, by (1) choosing a residence time  $\tau$ , (2) calculating  $J$  and  $\lambda$ , and (3) calculating  $X_{ss}$  and ( $R_{ss}/M_{in}$ ). Each calculation yielded a point on the curve for constant  $\psi$ . The calculations were continued up to the critical value of  $X_{ss}$  where the monomer droplets vanish  $f$ . As conversion increases,  $\tau$  is increasing along a curve of constant  $\psi$ . When monomer droplets remain in the system,  $\phi_m$  is constant and  $\lambda$  increases monotonically with  $\tau$ .

The peak of the curves of constant  $\psi$  is at the conversion where the droplets vanish. For conversions greater than  $f$ ,  $\phi_m^H$  changes with conversion, and the computational scheme to generate numerical values of ( $R_{ss}/M_{in}$ ) versus ( $X_{ss}$ ) was iterative. What developed for values of  $X_{ss}$  greater than  $f$  was that  $J^H$  and  $\lambda^H$  decreased with increasing values of  $\tau$ . This phenomenon was a result of the change in the value of  $K_G^H$  with  $\phi_m^H$ . One interesting feature of these results is that while Ley and Gerrens<sup>15</sup> postulated the existence of multiple steady states, our work showed the steady-state rate  $R_{ss}$ , and conversion  $X_{ss}$  to be single-valued functions of  $\tau$ . There are no choices of  $\tau$  which can result in a multiplicity of steady states. These results are a consequence of our assumption of a constant termination rate constant  $k_t$ . Kirillov and Ray<sup>21</sup> were able to demonstrate that

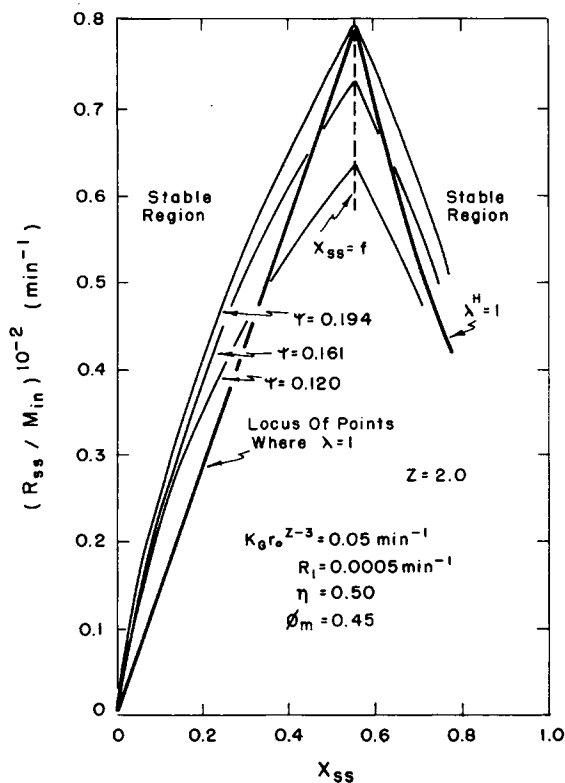


Fig. 4. Steady-state polymerization rate versus conversion showing stability envelope for  $z = 2.0$ .

multiple steady-state behavior arises as a result of the gel effect at high conversions for some situations.

The lines crossing the curves of constant  $\psi$  were constructed by connecting the points along the curves where  $\lambda$  (or  $\lambda^H$ ) was equal to unity. Points above this curve have  $\lambda < 1$ , and everywhere inside the envelope we have  $\lambda > 1$ .

From these figures one can understand the effects of changes in certain key independent parameters. The conclusions reached are dependent on whether or not monomer droplets remain in the system.

Increasing the value of  $\psi$  (proportional to  $S_{\text{eff}}$ ) can serve to guarantee stability. This effect could be realized by increasing the feed level of soap and is independent of the presence of monomer droplets.

Increasing  $\tau$  tends to push the system toward the unstable envelope when monomer droplets are present. The reverse is true when droplets do not exist.

At fixed  $\tau$ ,  $\lambda$  may be increased by increasing the feed concentration of initiator. Thus the same tendencies would result from increasing the initiator concentration in the feed as for increasing  $\tau$ .

Some of the results in the literature can be interpreted in the context of the results of this analysis. These are discussed below.

Gershberg and Longfield<sup>5</sup> showed that oscillatory behavior could be induced in their continuous styrene polymerizer by simply raising the temperature from

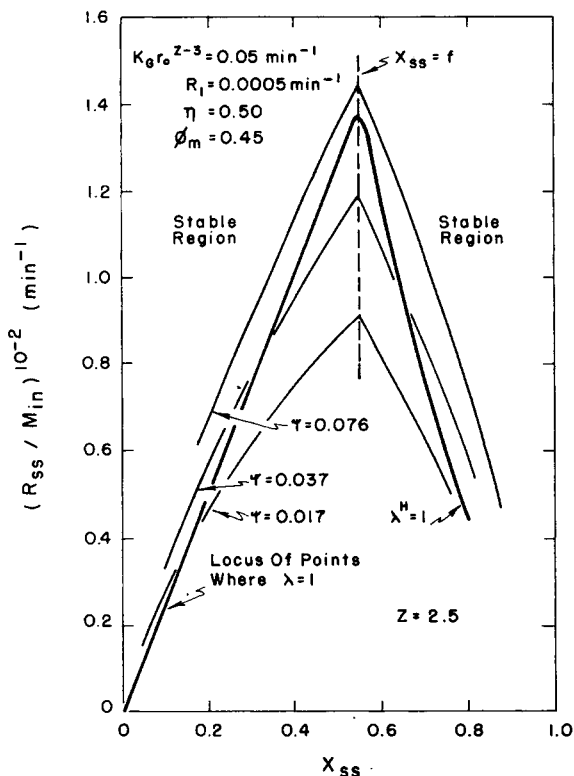


Fig. 5. Steady-state polymerization rate versus conversion showing stability envelope for  $z = 2.5$ .

70 to 100°C, with all other conditions the same. The consequence of the temperature elevation was to increase the initiator decomposition rate 30-fold, while the particle growth rate only increased by a factor of 4. This change of temperature has the same effect as increasing the feed concentration of initiator  $I_{in}$ , which our analysis shows should move the system toward the unstable region.

Omi et al.<sup>13</sup> predicted that increasing  $I_{in}$  or decreasing  $S_{in}$  increases the tendency of unstable operation. These predictions are consistent with our analysis.

Ley and Gerrens<sup>15</sup> observed oscillatory behavior in the continuous emulsion polymerization of styrene. They noted that their system was not stabilized by increasing  $I_{in}$  or  $S_{in}$  independently, but was stabilized by increasing both concentrations simultaneously. Noting that their experiments were at high conversion, we again point out consistency in the trends observed and predictions from this analysis. The fact that increasing  $I_{in}$  or  $S_{in}$  separately did not stabilize the system suggests that the system had initially been operating at a point so far into the unstable region that a single corrective action was not sufficient to remedy the situation.

Berens<sup>16</sup> noted fluctuations in the particle size distribution in his continuous emulsion polymerization of vinyl chloride, even though the monomer conversion appeared to be steady. He noted that seeding the polymerizer with latex particles stabilized the system. This tendency is consistent with the arguments presented earlier in this development.



Greene et al.<sup>17</sup> showed experimental results of the continuous emulsion polymerization of vinyl acetate and methyl methacrylate. Oscillatory behavior was observed in the effluent stream in both systems. They found that the tendency toward unstable operation was enhanced by increasing either  $I_{in}$  or  $\tau$ , consistent with our predictions. While changing  $S_{in}$  did not appear to result in definite trends in the ultimate monomer conversion attained, their system did tend toward unstable performance as  $S_{in}$  was decreased. These results are consistent with our predictions. From the observations they made they speculated that the instabilities result from the nucleation step and the gel effect. At the moderate monomer conversion levels of their experiments, one would not expect the gel effect to be of much significance, however. Undoubtedly the primary cause of the unstable operation in their system was the unstable nucleation mechanism. They confirmed this postulate by minimizing the instabilities when a prereactor was used to generate seeds.

## CONCLUSIONS

A population balance for the emulsion polymer particles based on the particle age distribution was used to generate transient expressions for various relevant properties of the latex in the continuous reactor. A nucleation function was used to describe the birth of new polymer particles. A growth rate expression was incorporated to relate the volumetric growth rate of particles to environmental conditions in the reactor. A relation of the form  $\bar{n} = Kr^z$  was included to relate the volumetric growth rate of particles to particle size.

The Laplace transform of the linearized population balance expressions indicated that the stability of the entire system is governed by the stability of the particle formation mechanism. Specifically, the analysis showed that unstable performance ought to result when the total polymer particle surface area in the reactor is more than half of what the incoming soap can cover. This result was the same irrespective of the choice of  $z$  in the growth rate expression. Results showed that when the polymer particle surface area was greater than half that which the incoming soap could cover the rate of particle nucleation was reduced, and partial washout of the existing particles must occur before a shower of new particles can be generated. These conditions led to oscillatory reactor performance. An analysis of the moments of the distribution indicated that for some values of  $z$  the continuous emulsion polymer reactor is always stable.

The analysis indicated that increasing the feed level of free radical initiator or the residence time would increase the tendency toward unstable performance when monomer droplets are present. However, increasing  $I_{in}$  or  $\tau$  after monomer droplets had vanished tended to stabilize the system. The analysis also indicated that the system may always be stabilized by increasing the feed concentration of emulsifier.

This study was carried out in regions of low conversion (where monomer droplets exist) and high conversion (where monomer droplets no longer exist). Only one steady-state operating point was found, contrary to previous work reported in the literature. This result is probably due to the assumption that the termination rate constant was assumed to be independent of conversion.

## APPENDIX

Some specific terms and relationships are defined here for the benefit of the reader.

Deviation variables are denoted with a prime. The deviation of the birth rate from the steady-state value, for example, is given by

$$B'(t) = B(t) - B_{ss} \quad (\text{A1})$$

Similarly, the deviation of the particle age density is

$$N'(t, \theta) = N(t, \theta) - N_{ss}(\theta) \quad (\text{A2})$$

which, when combined with eqs. (3) and (A1), gives

$$\begin{aligned} N'(t, \theta) &= B'(t, \theta)e^{-\theta/\tau} \quad \text{for } \theta \leq t \\ &= N_0(\theta - t)e^{-t/\tau} - B_{ss}e^{-\theta/\tau} \quad \text{for } \theta \geq t \end{aligned} \quad (\text{A3})$$

A cumulative property of the latex (particle surface area, particle volume, etc.) is found by summing up all the individual properties of the particles of all ages:

$$P(t) = \int_0^\infty p(t, \theta)N(t, \theta) d\theta \quad (\text{A4})$$

Then the deviation of a cumulative property from the steady-state value may be found:

$$\begin{aligned} P'(t) &= P(t) - P_{ss} \\ &= \int_0^\infty p(t, \theta)N(t, \theta) d\theta - \int_0^\infty p(t, \theta)N_{ss}(\theta) d\theta \\ P'(t) &= \int_0^t p(t, \theta)B'(t, \theta)e^{-\theta/\tau} d\theta \end{aligned} \quad (\text{A5})$$

Equation (A5) was developed by assuming that

$$N_{ss}(\theta) = N_0(\theta) \quad (\text{A6})$$

The three lumped constants associated with the particle generation function presented in eq. (4) are defined below:

$$R_0 = \rho_0 h_m \quad (\text{A7})$$

$$R_1 = \rho_0(h_m + h_h L/4) \quad (\text{A8})$$

and

$$S_{\text{eff}} = S - (cmc) - \frac{(A_{\text{drop}} - h_h/h_m)s_m}{a_m} \quad (\text{A9})$$

Three of the principal lumped parameters used in this work are defined below:

$$K_G = \frac{(3 - z)k_p \rho_m \phi_m K}{4\pi N_A \rho_p (1 - \phi_m)} \quad (\text{A10})$$

$$J = K_G \tau r_0^{(3-z)} \quad (\text{A11})$$

$$\lambda = 4\pi r_0^2 R_1 \tau \Gamma\left(\frac{5-z}{3-z}\right) e^{1/J} J^{2/(z-3)} \quad (\text{A12})$$

The constants just defined are applicable for  $0 \leq z < 3$ . For  $z = 3$ , new constants would need to be developed, due to the exponential dependence of particle radius to particle age [see eq. (8)]. While we have not presented the details of the solution for  $z = 3$ , the procedure would follow exactly as we have shown for  $z \neq 3$ , and the results are obtainable analytically for the steady state and the transient cases.

The constant  $\beta_\xi$  introduced in eq. (40) is defined as

$$\beta_\xi = \frac{\phi_\xi r_0^{\xi-2} (R_0 a_m / s_m) \bar{D}}{4\pi R_1 \tau \Gamma(-a)} \cdot \frac{J^{\xi/(3-z)}}{J^{2/(3-z)}} \left( 1 + \frac{\xi}{3-z} \right) \quad (\text{A13})$$

The parameter  $\psi$  used in Figs. 4 and 5 is given by

$$\psi = S_{\text{eff}} \rho_m \phi_m \nu_0 / s_m M_{\text{in}} M_w \quad (\text{A14})$$

The constants used in eq. (53) are defined by

$$\alpha = k_p \tau \rho_m \phi_m K / 4\pi N_A \rho_p (1 - \phi_m) \quad (\text{A15})$$

$$\epsilon = (a_0 R_0 \tau) (S_{\text{eff}} / s_m) \quad (\text{A16})$$

$$\sigma = a_0 R_1 \tau \quad (\text{A17})$$

## NOTATION

$A_T$	cumulative polymer particle surface area
$A_{\text{drop}}$	surface area of emulsified droplets
$A_m$	effective surface area of incoming soap
$(AR)$	amplitude ratio
$a$	constant = $(z - 5)/(3 - z)$
$a_0$	surface area of a particle nucleus
$a(\theta)$	surface area of particles of age $\theta$
$a_m$	surface area of a micelle
$B(t)$	particle nucleation function
$(cmc)$	critical micelle concentration
$D$	a disturbance in the soap level
$f$	mass fraction of monomer in particles when droplets vanish
$G$	radial growth rate of particles
$G(s)$	surface area-related transfer function in nucleation function
$h_h$	fraction of radicals which initiate polymerization in the continuous phase
$h_m$	fraction of radicals which initiate polymerization in micelles
$I$	initiator concentration
$J$	lumped parameter defined in eq. (A11)
$K$	constant associated with size-dependent average number of free radicals per particle
$K_G$	lumped constant defined in eq. (A10)
$L$	critical diffusion length
$\bar{L}$	number average radius of polymer particles
$M$	effluent monomer concentration
$M_i(t)$	time-dependent $i$ th moment of distribution
$M_w$	molecular weight of monomer
$N_A$	Avogadro's number

$N_T$	total number of particles per volume of latex
$N_0(\theta)$	initial age density of particles
$N(t, \theta)$	number density of particles per volume of latex per unit age
$\bar{n}(\theta)$	average number of free radicals per particle of $\theta$ -aged particles
$P(t)$	a characteristic latex property; summed over all particles
$p(t, \theta)$	a characteristic particle property; depends on particle age
$R$	polymerization rate
$R_0$	constant defined in eq. (A7)
$R_1$	constant defined in eq. (A8)
$r(\theta)$	radius of particles of age $\theta$
$S$	soap concentration
$S_{\text{eff}}$	effective concentration of soap available for particle nucleation
$s$	dimensionless-independent time variable in the Laplace domain
$s_m$	amount of soap in a micelle
$T$	dimensionless time ( $t/\tau$ )
$U(r)$	particle size distribution function
$\bar{u}(r)$	cumulative particle size distribution
$V_T$	cumulative polymer particle volume
$v(\theta)$	volume of particles of age $\theta$
$X$	monomer conversion
$z$	constant exponent relating average number of radicals per particle to particle radius
$\alpha$	combined constant defined in eq. (A15)
$\beta_\xi$	combined constant defined in eq. (A13)
$\delta$	standard deviation of radial particle size distribution
$\epsilon$	combined constant defined in eq. (A16)
$\xi$	constant relating particle property to particle radius; eq. (38)
$\rho_0$	free radical production rate
$\rho_m$	monomer density
$\rho_p$	polymer density
$\sigma$	combined constant defined in eq. (A17)
$\eta$	mass fraction of monomer in particles
$\theta$	age of a polymer particle
$\lambda$	combined constant defined in eq. (A12)
$\mu_i(t)$	time-dependent normalized $i$ th moment
$\tau$	average reactor residence time
$\Phi$	phase lag
$\phi_m$	volume fraction of monomer in particles
$\phi_\xi$	shape factor relating particle property to particle radius; eq. (38)
$\psi$	dimensionless constant defined in the Appendix
$\omega$	independent variable in the Laplace domain

### *Subscripts*

in	inlet conditions
ss	steady-state conditions
0	evaluated at micelle size (unless otherwise noted)

*Superscripts*

- H* high conversion; no monomer droplets exist  
 ' "prime," deviation variables  
 - "tilde," dependent variables in Laplace domain

The computer time for this study was provided without charge by WACCC at W.P.I. The authors would like to express appreciation to Professor A. E. Hamielec for providing us with an early copy of his manuscript. We also wish to acknowledge the helpful comments provided by Professor G. W. Peohlein.

**References**

1. W. D. Harkins, *J. Am. Chem. Soc.*, **69**, 1428 (1947).
2. W. V. Smith and R. H. Ewart, *J. Chem. Phys.*, **16**, 592 (1948).
3. J. Ugelstad and F. K. Hansen, *Rubber Chem. Technol.*, **49**, 536 (1976).
4. D. C. Blackley, *Emulsion Polymerization: Theory and Practice*, Wiley, New York, 1975.
5. D. B. Gershberg and J. E. Longfield, unpublished paper presented at the Symposium on Polymerization Kinetics and Catalyst Systems, 54th AIChE Meeting, New York, preprint No. 10, 1961.
6. T. Sato and I. Taniyama, *Kogyo Kagaku Zasshi*, **68**, 67 (1965).
7. T. Sato and I. Taniyama, *Kogyo Kagaku Zasshi*, **68**, 106 (1965).
8. R. W. Thompson and J. D. Stevens, *Chem. Eng. Sci.*, **30**, 663 (1975).
9. A. W. DeGraff and G. W. Poehlein, *J. Polym. Sci., Part A2*, **9**, 1955 (1971).
10. J. D. Stevens and J. O. Funderburk, *Ind. Eng. Chem., Process Des. Dev.*, **11**, 360 (1972).
11. K. W. Min and W. H. Ray, *J. Macromol. Sci., Rev. Macromol. Chem.*, **C11**, 177 (1974).
12. R. W. Thompson and J. D. Stevens, *Chem. Eng. Sci.*, **32**, 311 (1977).
13. S. Omi, T. Ueda, and H. Kubota, *J. Chem. Eng. Jpn.*, **2**, 193 (1969).
14. H. Gerrens and K. Kuchner, *Br. Polym. J.*, **2**, 19 (1970).
15. G. Ley and H. Gerrens, *Makromol. Chem.*, **175**, 563 (1974).
16. A. R. Berens, *J. Appl. Polym. Sci.*, **12**, 251 (1974).
17. R. K. Greene, R. A. Gonzalez, and G. W. Poehlein, Putma and Gardon, eds., *ACS Symp. Ser.*, **24**, 341 (1976).
18. A. S. T. Chiang, M.S. Thesis, Worcester Polytechnic Institute (1978).
19. C. Kiparissides, J. F. McGregor, and A. E. Hamielec, *J. Appl. Polym. Sci.*, **23**, 401 (1979).
20. A. S. T. Chiang and R. W. Thompson, *AIChE J.*, **25**, 552 (1979).
21. V. A. Kirillov and W. H. Ray, *Chem. Eng. Sci.*, **33**, 1499 (1978).
22. A. D. Randolph and M. A. Larson, *Theory of Particulate Processes*, Academic Press, New York, 1971.
23. J. L. Gardon, *J. Polym. Sci. Part A1*, **6**, 623 (1968).
24. R. M. Fitch and C. H. Tsai, in *Polymer Colloids*, R. M. Fitch, Ed., Plenum, New York, 1971.
25. J. W. Vanderhoff, J. F. Vitkuske, E. B. Bradford, and T. Alfrey, *J. Polym. Sci.*, **20**, 225 (1956).
26. G. W. Poehlein and J. W. Vanderhoff, *J. Polym. Sci., Polym. Chem. Ed.*, **11**, 447 (1973).
27. N. Friis and A. E. Hamielec, *J. Polym. Sci., Polym. Chem. Ed.*, **12**, 251 (1974).

Received April 27, 1979